

Universality in active chaos

Tamás Tél

Institute for Theoretical Physics, Eötvös University, P.O. Box 32, H-1518, Budapest, Hungary

Takashi Nishikawa*

Department of Mathematics, Southern Methodist University, Dallas, TX 75275, USA

Adilson E. Motter

*Max Planck Institute for the Physics of Complex Systems,
Nöthnitzer Strasse 38, 01187 Dresden, Germany*

Celso Grebogi

Instituto de Física, Universidade de São Paulo, Caixa Postal 66318, 05315-970, São Paulo, SP, Brazil

Zoltán Toroczkai

Complex Systems Group, Theoretical Division, Los Alamos National Laboratory, MS B213, Los Alamos, NM, 87545, USA

Many examples of chemical and biological processes take place in large-scale environmental flows. Such flows generate filamental patterns which are often fractal due to the presence of chaos in the underlying advection dynamics. In such processes, hydrodynamical stirring strongly couples into the reactivity of the advected species and might thus make the traditional treatment of the problem through partial differential equations difficult. Here we present a simple approach for the activity in in-homogeneously stirred flows. We show that the fractal patterns serving as skeletons and catalysts lead to a rate equation with a universal form that is independent of the flow, of the particle properties, and of the details of the active process. One aspect of the universality of our approach is that it also applies to reactions among particles of finite size (so-called inertial particles).

Keywords: reaction, Lagrangian chaos, filamental fractal, inertial effect

Environmental processes of biological and chemical nature, like the plankton blooming in the oceans[1, 2] and the ozone depletion in the stratosphere[3, 4], occur within fluid flows. The study of such processes is of importance in a broad range of fields including chemistry[5, 6, 7, 8, 9], population dynamics[10], geophysics, atmospheric sciences[11, 12, 13] and combustion[14]. Many chemical and biological species are immersed in a dynamic environment typically characterized by a time-dependent flow which advects and stirs the species. Because the advection dynamics is often (Lagrangian) chaotic, the application of the theory of dynamical systems to hydrodynamical advection problems [15, 16, 17] sheds new light on the reactive dynamics and on the production efficiency in such flows. As a result of the chaotic dynamics, fractal patterns are present, and the product distribution of the reactive process becomes concentrated along these patterns. There is evidence that such a filamental structure is indeed present in the distribution of active species in oceanic and atmospheric flows, such as the one shown in Fig. 1. In this article, we develop a description for active processes in flows with such structure. Our results imply that the character of a reaction can drastically change if it takes place in a time-dependent flow. A reaction which spreads over the whole space in a well mixed container



figure1.jpg

FIG. 1: Filamentation in a phytoplankton bloom in Norwegian Sea. (Provided by the SeaWiFS Project, NASA/Goddard Space Flight Center, and ORBIMAGE, URL: <http://visibleearth.nasa.gov/cgi-bin/viewrecord?5278>)

*Electronic address: tnishi@smu.edu

can lead to a pattern formation of a new type: the product is asymptotically distributed around a filamental fractal which moves in a rhythm corresponding to the time dependence of the flow. In a periodic case, the total amount of product is thus oscillating around a mean: a kind of limit-cycle behavior sets in. This pattern formation is due to the interplay of the chaotic particle motion produced by hydrodynamics and the production of the new particles by the reaction. In particular, we show that the theory is also valid if the reaction takes place with inertial particles, i.e., with particles of small but finite size whose density differs from that of the surrounding fluid.

A standard approach to describe active processes in flows is based on the use of advection-reaction-diffusion equations. The basic required assumption, from the Eulerian hydrodynamical point of view, is that *the active species behave as fluid particles*, and as such, their distribution can faithfully be described by smooth concentration fields. As a simple example, consider an auto-catalytic reaction $A + B \rightarrow 2B$ in which an unlimited amount of component A is present. In a homogeneously mixed environment, the reaction equation is $db/dt = kab$, where a and b stand for the respective A and B concentrations and k is the reaction rate. If the concentrations of A and B are not homogeneous in space, diffusion plays a role, and the reaction outcome is described by a partial differential equation:

$$\frac{\partial b}{\partial t} + (\mathbf{u} \cdot \nabla)b = kab + \kappa \Delta b, \quad (1)$$

where κ is the diffusion coefficient and \mathbf{u} is the velocity of the fluid (and a is the fixed concentration of the component A). This is the advection-reaction-diffusion equation, in which the presence of the advection term $(\mathbf{u} \cdot \nabla)b$ indicates that, in this approach, the advection of particles must take part with the fluid velocity \mathbf{u} . Although this approach is capable of describing a filamentation process[18, 19, 20, 21], it might break down if strong clusterization takes place [22, 23] as in the case where inertial effects of the advected reacting particles are included.

Inertial effects are due to the fact that the active particles are *of finite size*, and they can be *heavier or lighter* than the fluid. This is the case with aerosol particles or cloud rain droplets[24] in the air (heavier) and with gaseous bubbles in fluids or some species of phytoplankton in oceans (lighter). Such particles, due to viscosity (Stokes drag), try to follow the surrounding fluid, but typically diverge from the fluid trajectory[25, 26, 27, 28, 29, 30, 31, 32, 33, 34, 35]. The inertial effect alone is a source of chaotic behavior[27, 36, 37, 38]. In general, because of viscosity, the dynamics of inertial particles is dissipative and it is characterized by the presence of attractors. An attractor embodies the general tendency towards accumulation or clusterization of inertial particles (see Appendix A). As a result, the advection-reaction-diffusion equation (1) *is no longer valid* for the inertial active particles since the particle motion differs from that of the surrounding fluid. A partial description in terms of concentration is available, but only for the continuity equation and the diffusion equation[39, 40], or in the limit of small inertia[30, 41], which can only be a starting point for more general problems. At present, it is unknown whether an equation, analogous to Eq. (1), exists at all for active inertial particles. This fact alone calls for an alternative description of the global kinetics of the active species.

Herewith we present an approach that can successfully be applied to describe the kinetics of active particles in a flow. The idea is to determine the total number of particles of a given constituent in a macroscopic range of the fluid after some time, and show that this quantity fulfills a kind of simple rate equation.

The essential ingredient of our theory is the existence of a fractal dimension D in the physical space of the fluid for the reaction-free advection problem. This fractality means that, after some transient time (reacting or non-reacting) particles accumulate along zero-width filaments of a D -dimensional fractal set in the fluid. There are some pieces of evidence that suggests the presence of such filamental fractal sets in a variety of processes taking place in flows[1, 2, 3, 4, 5, 6, 7, 8, 9, 10, 11, 12, 13, 14]. There are two distinct dynamical origins for such fractal sets. The better known of them is the presence of a *chaotic attractor*[27, 32, 33, 34, 35, 36, 37, 38] in the inertial problems. The other possibility is for the advection dynamics to exhibit *transient chaos*[42, 43, 44, 45], which can be associated with chaotic saddles in the advection dynamics of either the inertial or noninertial problems. The fractal filaments align along the unstable direction, where stretching takes place, and across these filaments, contraction occurs. In typical chaotic systems, this contraction is exponential in time with some contraction rate $\lambda > 0$. In the language of dynamical system theory, $-\lambda$ is the largest among the contracting Lyapunov exponents of the advection dynamics which, of course, depends on the flow's hydrodynamical characteristics and the particle's inertial properties. This means that a typical distance of δ across the filaments shrinks with a velocity $-\lambda\delta$.

In what follows we restrict our attention to autocatalytic reactions which occur often in nature[6]. For such processes, the reaction typically propagates in the form of fronts (the stable B phase propagates into the unstable A phase) with relatively sharp boundaries, since the effect of diffusion is rather weak on the length scales of interest[46]. In the simplest approximation, both ozone depletion and plankton blooming can be described by front propagation of this type. Further examples are the Belousov-Zhabotinskii reaction[47] and the propagation of flames[48].

Many real examples of environmental flows are essentially two dimensional, and thus we restrict ourselves here to the case where D is between 1 and 2. The flow has a clean fractal structure when D is well defined and it is different from both 1 and 2. We note, however, that a similar treatment is applicable even to a three-dimensional flow with

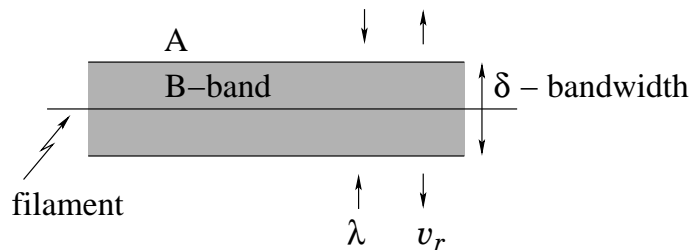


FIG 2. Tel CHAOS

FIG. 2: Local reaction-advection dynamics on a filamental segment.

fractal invariant manifolds, since the arguments below are quite general.

Consider a blob of B-particles in a region of interest. After some time, material B will be distributed along filaments in bands of average width δ . Consider now a *single* filamental segment on the underlying fractal, covered by a band of B-particles with the average width of δ , as illustrated in Fig. 2. The width of the band decreases at the rate $-\lambda\delta$ but there is, due to the reaction, also an increase of it. Approximating the local reaction front velocity by its average value v_r , the rate of increase of the width is $2v_r$. Thus, the time derivative $\dot{\delta} \equiv d\delta/dt$ of the width is given as

$$\dot{\delta} = -\lambda\delta + 2v_r. \quad (2)$$

This simple differential equation expresses the competition of two effects: the exponential contraction towards the underlying fractal, and the linear expansion due the autocatalytic process, which could be regarded as a kind of “infection”. After some transient time, this competition leads to a steady state ($\dot{\delta} = 0$) characterized by the fixed point value $\delta^* = 2v_r/\lambda$.

The basic observation is that on any filamental segment accumulates infinitely many other segments, since they form a fractal set. However, after the spreading of the material along any one of these fractal segments, there is a fattening up of the segments and we can assume that these bands are similar to the typical one just been treated above and have bandwidth δ . Then, the number of B-particle bands *observed* to cover the segments with an average instantaneous width δ is finite. The union of all bands of B-particles, covering the fractal filaments, appears to be a fractal on length scales above δ , but it is a two-dimensional object below this crossover scale. Let us consider a fixed region that contains the filamental fractal bands. According to the fractal geometry[49, 50], the minimal number N of boxes needed to cover a fractal set of dimension D with boxes of linear size ε is proportional to ε^{-D} . By using the actual width δ of the B-coverage as the box size ($\varepsilon = \delta$), the number of boxes needed to cover the fractal filaments in the region of observation is $N(\delta) \sim \delta^{-D}$. The symbol \sim indicates the presence of a proportionality geometric factor not written out explicitly. The total area covered by the B-particles is therefore $N(\delta)$ times the area δ^2 of a single box, or $\delta^2 N(\delta)$, which is proportional to δ^{2-D} . Although the number of B-particles in each box may vary along the filaments due to the stretching and folding action of the advection dynamics, the average number of particles in each box will saturate, since the number of A-particles available in each box is limited. It is then natural to assume that the area δ^{2-D} is proportional to the *number* B of the B-particles in a given region of observation, i.e., $B \sim \delta^{2-D}$. The time derivative of the total number of B-particles is $\dot{B} \sim (2 - D)\delta^{1-D}\dot{\delta}$, where $\dot{\delta}$ can be obtained simply by substituting it from (2). Thus, \dot{B} can be written as the sum of a (negative) loss term $-L$ and a (positive) production term P :

$$\dot{B} = P(B) - L(B), \quad (3)$$

where

$$L(B) = \lambda(2 - D)B, \quad P(B) = cv_r(2 - D)B^{-\beta} \quad (4)$$

with c as a B -independent geometric factor (which might depend on the location and the size of the region of observation), and

$$\beta \equiv \frac{D - 1}{2 - D}. \quad (5)$$

The exponent of the production term is always negative since $1 < D < 2$ (β is positive). Thus, the overall structure of the rate equation is

$$\dot{B} = -c_1 B + c_2 v_r B^{-\beta},$$

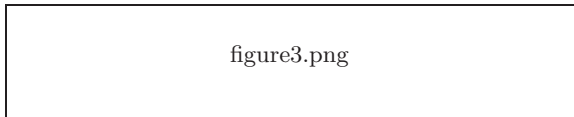


FIG. 3: Autocatalytic inertial particles advected by a two-dimensional flow field of counter-rotating array of vortices with time-periodic intensity[27], given by the stream function (6) with $\omega = \pi$. The flow can be regarded as a model of the arrangement of eddies in a vertical plane of the lower atmosphere or the upper ocean. The parameter k measures the amplitude of oscillation of the strength of the vortices. (a), (b) Chaotic sets in the advection dynamics of the nonreacting inertial B-particles: (a) chaotic attractor ($k = 0.53$) and (b) chaotic saddle responsible for transient chaos ($k = 0.524$). The small rectangle at the top of the panel (b) is magnified in the inset to show the small scale (Cantor-like) structure of the saddle. The other parameters are $St = 1$, $\alpha = 1.7$, and $w = -3.934$ (see Appendix A). (c), (d) Distribution of the product particles after a sufficiently long time ($t = 100$ periods of the flow field). Fractal filamentation is caused by the chaotic attractor in (c) and by the chaotic saddle in (d). Only a single vortex cell of $[0, \pi] \times [0, \pi]$ is shown and the gravity points downward in (a)-(d). The color coding represents the density of B-particles, in which darker colors correspond to higher density. The density of B-particle is bounded in this simulation[36]. Note that in (d) the product is distributed not along the chaotic saddle but along its unstable manifold [the difference between the saddle in (b) and the unstable manifold seen in (d) is apparently small, partly because they are projected onto the two-dimensional configuration space]. The initial condition is a small blob of B-particles. (e), (f) The total number B^* of the B-particles in the steady state vs the reaction velocity v_r in the case of the chaotic attractor in (e) and the chaotic saddle in (f). The full line corresponds to the fit $B^* \sim v_r^{2-D}$ predicted by the theory [see Eq. (8)]. For reference, the $B^* \sim v_r$ line is shown as a dashed line, which corresponds to a nonchaotic case ($D = 1$).

where c_1 and c_2 are positive coefficients independent of the reactive process. The novel feature of this equation is the singularity of the term $P(B)$. It states that the smaller is the number of B-particles, the higher is the production. This peculiar scaling property of the production term has been verified in numerical simulations for autocatalytic noninertial particles[44, 45, 46]. Here we emphasize that these results are *valid for inertial particles* as well. Figure 3 shows the results of the numerical simulations for finite-size active B particles in a simple two-dimensional cellular flow field, given by the stream function

$$\psi(x, y) = [1 + k \sin(\omega t)] \sin x \sin y, \quad (6)$$

where k and ω are the amplitude and angular frequency of the temporal oscillation of the flow field, respectively[36, 37, 38].

The universality of our description is grounded on the generic property of a filamental fractal that the perimeter length of its finite-width coverage *increases* as the area of coverage decreases. This relationship leads to singularly enhanced reactivity. In order to see this, let us derive the relationship between the observed perimeter length \mathcal{L} and the area \mathcal{A} of filamental fractals. Since the covering of such a fractal set with small squares of linear size ε requires $N(\varepsilon) \sim \varepsilon^{-D}$ such squares, and since two of the four edges of each box typically belong to the perimeter of the coverage, the perimeter length is proportional to ε^{1-D} and *increases* with refining resolution ($D > 1$) (see Fig. 4). On the other hand, the area is proportional to ε^{2-D} and *decreases* with refining resolution ($D < 2$). By eliminating ε from the relations $\mathcal{L} \sim \varepsilon^{1-D}$ and $\mathcal{A} \sim \varepsilon^{2-D}$, we find that

$$\mathcal{L} \sim \mathcal{A}^{-\beta} \quad (7)$$

with β as given by (5). Thus, the perimeter length is, at any small resolution, a *negative* power ($-\beta$) of the area [51]. (Note that for classical nonfractal objects, e.g., a sphere or a cube, one has $\mathcal{L} \sim \mathcal{A}^{1/2}$, which is non-singular since the exponent is positive.) In view of this, the production term P in (3) can be interpreted as the expression for the fact that the reaction takes place along the perimeter of the fattened-up filamental fractal seen at resolution δ . Since the peculiar relationship (7) is purely geometrical, it does not depend on the precise nature of the activity. Similar singular terms appear in the equation for other types of activity as well[44, 45].

In summary, the fractal filaments of the advection problem act as dynamical *catalysts* for the reactions. The rate equation (3) has a *universal* character, as its form does not depend either on the particle, flow or reactivity properties. Fundamentally, the exponent β characterizes the geometry of the reaction-free chaotic advection. The singular productivity disappears for $D = 1$, representing a flow in which the filaments do not form a fractal, and the advection is consequently nonchaotic.

Equation (3) describes the competition of two effects: contraction and production. As a result of the balance between these effects, a *steady state* sets in after sufficiently long time for the global distribution of the B-particles [see Figs. 3(c) and 3(d)]. This steady state is synchronized to the flow, i.e., it takes over the time dependence of the flow and in general follows the hydrodynamical time dependence manifested in the parameter c . In the case when the

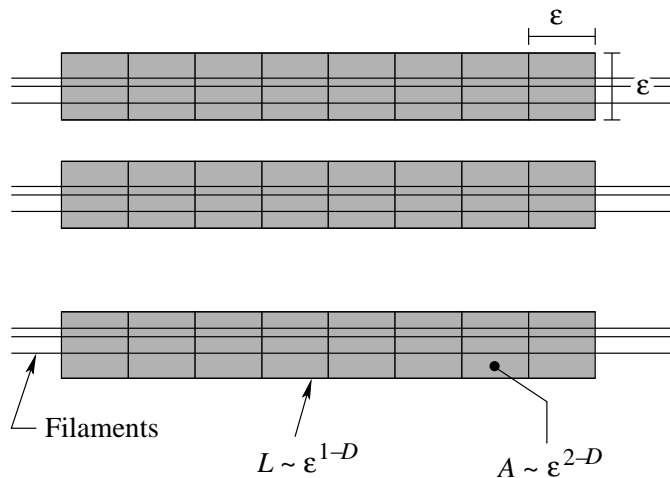


FIG 4. Tel CHAOS

FIG. 4: Schematic diagram illustrating the ε -dependence of the perimeter length \mathcal{L} and the area \mathcal{A} of a filamental fractal, when observed with resolution ε .

time dependence of parameter c is weak, the steady state value of the number of particles is

$$B^* = \left(\frac{cv_r}{\lambda}\right)^{2-D} \sim \delta^{*2-D}. \quad (8)$$

The scaling is unique: B^* is proportional to the power $(2 - D) < 1$ of the reaction velocity. This means that the number B^* of particles decreases by a factor smaller than the factor by which the reaction velocity decreases. For example, if $v_r \sim 10^{-4}$, the value of B^* with $D = 1.5$ is two orders of magnitude larger than that for the traditional active process where $D = 1$. Equation (8) is confirmed in Figs. 3(e) and 3(f) for inertial particles whose dynamics possesses a chaotic attractor and transient chaos, respectively.

Remark I: Production vs diffusivity. Because the reaction front velocity v_r is known[52, 53] to be proportional to the square root of the diffusion coefficient κ , we obtain from (8)

$$B^* \sim \kappa^{1-D/2}.$$

The amount of particles produced is proportional to the fractional power $(1 - D/2)$ of the diffusion coefficient. This relation for diffusive particles has been derived using an Eulerian approach in [4, 12]. Our arguments herewith imply that it is in fact valid for active inertial particles as well, provided $v_r \sim \kappa^{1/2}$.

Remark II: Dependence of production on resolution. Let us now consider the production term P , but for simplicity, in the steady state. Assume that this production is measured with a resolution ε worse than the crossover scale length, i.e., $\varepsilon > \delta^*$. Since the production is proportional to the perimeter length seen with the resolution used, we have

$$P(\varepsilon) \sim \varepsilon^{1-D}. \quad (9)$$

The exact amount of production $P(\delta^*)$ is, however, proportional to δ^{*1-D} . The ratio of the observed, coarse-grained amount of production to the exact one is thus

$$\frac{P(\varepsilon)}{P(\delta^*)} = \left(\frac{\delta^*}{\varepsilon}\right)^{D-1}. \quad (10)$$

By improving the resolution (decreasing ε to δ^*) the ratio moves towards unity. This dependence is not present at all in the nonchaotic case where $D = 1$. Therefore, we conclude that the increase of productivity with increasing resolution observed earlier in simulations of environmental problems[3, 54] is describable by the equation derived in this paper. Our results show that this effect is present even when the description of the hydrodynamical flow field is complete, in contrast to the similar effect reported before[3, 54], which may be due to incomplete knowledge of the flow field. Although previous studies[3, 54] treat only noninertial particles, it follows from our approach that this behavior must be present in the inertial problem as well.

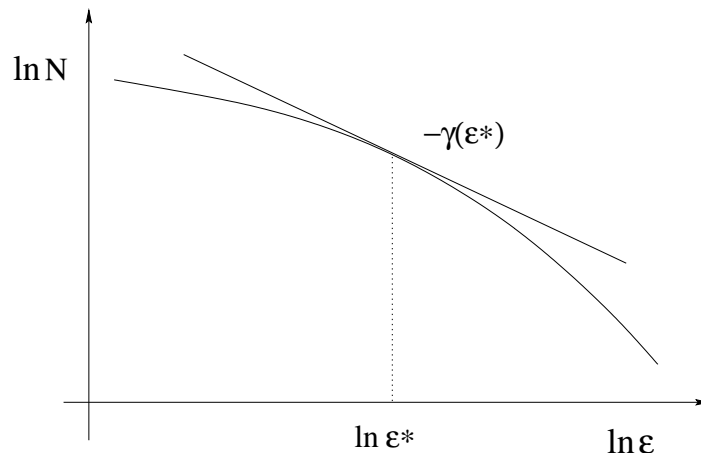


FIG. 5 Tel CHAOS

FIG. 5: The definition of the exponent $\gamma(\varepsilon^*)$ for a given resolution ε^* .

Remark III: Enhancement factor. In a nonchaotic flow, the average width δ^* of B-particle bands in the steady state is proportional to v_r/λ . The enhancement factor relative to the nonchaotic case is thus

$$\frac{B^*(D)}{B^*(D=1)} \cong \left(\frac{v_r}{\lambda}\right)^{1-D}. \quad (11)$$

Since δ^* is typically much smaller than the characteristic length scale of the flow (chosen here to be unity), there is always a considerable enhancement due to the chaoticity of the advection dynamics (recall $1 - D < 0$) [55].

We emphasize that these results are independent of the nature of reaction (autocatalytic, bistable, excitable, etc.), that is, whenever the product is distributed in bands along filaments of a fractal set, Eqs. (3)–(11) hold.

Remark IV: Effects of nonfractal filaments. The existence of a well-defined fractal scaling over decades of resolution is actually not necessary for our theory to work. For systems close to the steady state, our approach only requires that $N(\delta)$ is a power law of δ at the length scale around δ^* . This is important because many filamental structures observed in environmental processes do not present a clear scaling over decades of resolution. This is the case, for example, for the plankton growth [10], or for the deactivation process of the ClO-rich polar air by the NO₂-rich air in the mid-northern latitudes, which can suppress the depletion of ozone [4]. Our treatment can be carried out in this case with an exponent $\gamma(\varepsilon = \delta^*)$ replacing D , where $\gamma(\varepsilon)$ is defined as the slope of the $\ln N(\varepsilon)$ vs $\ln(1/\varepsilon)$ curve (see Fig. 5):

$$\gamma(\varepsilon) = -\frac{d \ln N(\varepsilon)}{d \ln \varepsilon}.$$

The exponent γ is a quantity which would be the fractal dimension D if the exact scaling $N(\varepsilon) \sim \varepsilon^{-D}$ holds with a constant D . Equations (3)–(11) remain valid if we substitute

$$D \rightarrow \gamma(\delta^*).$$

Note, however, that, in contrast to the case of a clear fractality, the use of our theory in this case requires the knowledge of the steady state width δ^* and the assumption that B is close to its steady state value B^* so that $\gamma(\delta^*)$ stays approximately constant over time. We observe that the exponent γ , relevant for reactions, can be different from the exact dimension of an underlying fractal set, even when such a quantity exists (see Appendix B).

Conclusions: Starting from a particle-based “microscopic” picture, we derived, by applying elementary rules of the fractal geometry, a novel type of rate equation in which the production term does not follow the principle of “mass-action” [56] well known from thermodynamics. In fact, these processes are much further away from thermal equilibrium than traditional reactions since they do not fill the configuration (or phase) space. The problem treated here provides a clean example of a feature we believe to be general: whenever a transport process is concentrated on a fractal set in the configuration space, the corresponding *transport equation deviates substantially* from the one known from irreversible thermodynamics.

APPENDIX A: EQUATION OF MOTION FOR INERTIAL PARTICLES

For small spherical particles of finite size, the particle velocity $\mathbf{v} = d\mathbf{r}/dt$ (\mathbf{r} is the position of the particle) typically differs from the fluid velocity \mathbf{u} . The equation of motion is given by Newton's second law: the force causing the relative acceleration $d\mathbf{v}/dt - d\mathbf{u}/dt$ [$d\mathbf{u}/dt \equiv \partial\mathbf{u}/\partial t + (\mathbf{u} \cdot \nabla)\mathbf{u}$] between the particle and the fluid is due to the viscous friction and, in the gravitational field, due to buoyancy. The former, the so-called Stokes drag, is proportional to the velocity difference $\mathbf{v} - \mathbf{u}$, and vanishes for pointlike particles. The latter is proportional to the density difference $\varrho_{\text{particle}} - \varrho_{\text{fluid}}$. The dimensionless form of the equation of motion reads[25, 26, 39, 57]:

$$\frac{d\mathbf{v}}{dt} - \alpha \frac{d\mathbf{u}}{dt} = -\frac{\mathbf{v} - \mathbf{u}}{St} - w\mathbf{n}. \quad (\text{A1})$$

Here $St > 0$ is the Stokes number, the dimensionless decay time due to the Stokes drag, w (positive for heavy particles) is the dimensionless buoyancy force acting in the vertical direction, and \mathbf{n} denotes the vertical normal vector pointing upward. The coefficient $\alpha > 0$ expresses the fact that a finite size particle brings into motion a certain amount of fluid proportional to its volume. The noninertial particle dynamics is recovered when the particle radius vanishes, which corresponds to the limit $St \rightarrow 0$. In this limit, the advection dynamics is governed by

$$\mathbf{v} = \frac{d\mathbf{r}}{dt} = \mathbf{u}(\mathbf{r}, t).$$

The general inertial dynamics (A1) possesses a four-dimensional phase space (x, y, v_x, v_y) even for planar stationary flows, whereas for the non-inertial particle dynamics the phase space is two dimensional. The inertial dynamics is dissipative, even in incompressible flows, and the phase space volume contracts at the rate $-2/St$, which is always negative, in contrast to the noninertial case which is volume preserving. The fractal object in the full phase space must have a dimension less than 2, if one wishes to keep its fractality in the projection onto the configuration space of the flow.

APPENDIX B: DIFFERENCE BETWEEN $\gamma(\varepsilon)$ AND FRACTAL DIMENSION

An illustrative example where the exponent $\gamma(\varepsilon)$ differs from the fractal dimension is the case of point particles advected by a flow in which chaotic and regular motions coexist (the so-called nonhyperbolic dynamics). A transverse intersection between a line and the filamental fractal associated with such a chaotic motion can be modeled by a Cantor set constructed as follows. In the first step, an interval is removed from the middle of the unit interval. An interval is removed from each of the remaining two intervals in the second step. The third step removes intervals from the middle of all remaining interval, and so on. In contrast to the hyperbolic chaotic systems, the relative size of removed intervals at each step is not constant, but, for example, is inversely proportional to the number of steps in the construction[58]. In this case, the limit set in the two-dimensional space is a fractal set of dimension two. However, the exponent γ at resolution ε is smaller than 2 and can be approximated by

$$\gamma(\varepsilon) \approx 2 - \frac{1}{\ln(1/\varepsilon)}.$$

The exponent γ converges very slowly to the exact dimension 2 and it is quite different from the limiting value, even for unrealistically small scales, as shown in Fig. 6. A similar behavior for the exponent γ is also expected in the presence of small dissipation due to inertial effects[42, 43]. If a reactive process takes place in such a nonhyperbolic advection dynamics, D in (3)–(11) must be replaced by the exponent $\gamma(\varepsilon = \delta^*)$ in a self-consistent manner.

ACKNOWLEDGMENTS

This work was supported by the Hungarian Science Foundation (OKTA T032423) and the MTA/OTKA/NSF Fund (Project No. Int. 526). AEM and CG were supported by FAPESP, and CG was additionally supported by CNPq. ZT was supported by the DOE under contract No. W-7405-ENG-36. We thank Max-Planck-Institut für Physik

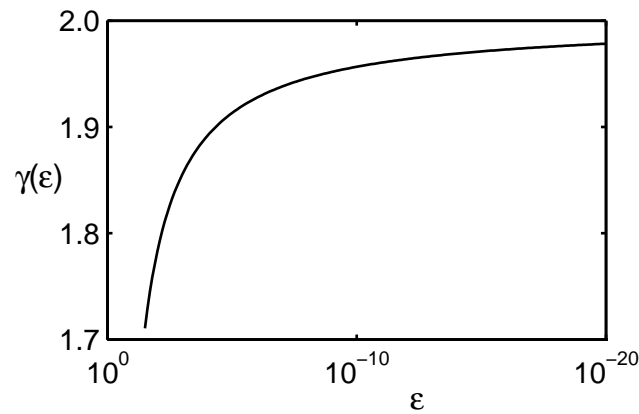


FIG. 6 Tel CHAOS

FIG. 6: The exponent γ as a function of the observational scale ε for the filamental fractal constructed in Appendix B, which models fractals observed in typical nonhyperbolic systems.

Komplexer Systeme, Dresden, Germany where some of the key ideas of this work were discussed.

-
- [1] E. R. Abraham, *Nature (London)* **391**, 577 (1998); A. Bracco, A. Provenzale, and I. Scheuring, *Proc. R. Soc. London, Ser. B* **276**, 1795 (2000); A. P. Martin, K. J. Richards, A. Bracco, and A. Provenzale, *Global Biogeochem. Cycles* **16**, 1025 (2002). A. P. Martin, *J. Plankton Res.* **22**, 597 (2000); *Prog. in Oceanogr.* **57**, 135 (2003);
- [2] E. R. Abraham, C. S. Law, P. W. Boyd, S. J. Lavender, M. T. Maldonado, and A. R. Bowie, *Nature (London)* **407**, 727 (2000).
- [3] S. Edouard, B. Legras, F. Lefevre, and R. Eymard, *Nature (London)* **384**, 444 (1996).
- [4] A. Wonhas and J. C. Vassilicos, *Phys. Rev. E* **65**, 051111 (2002).
- [5] G. Metcalfe and J. M. Ottino, *Phys. Rev. Lett.* **72**, 2875 (1994).
- [6] I. R. Epstein, *Nature (London)* **374**, 321 (1995).
- [7] O. Paireau and P. Tabeling, *Phys. Rev. E* **56**, 2287 (1997).
- [8] M. Menzinger and P. Jankowski, *J. Phys. Chem.* **90**, 1217 (1986); M. Menzinger and A. K. Dutt, *ibid.* **94**, 3410 (1990); F. Ali and M. Menzinger, *ibid.* **101**, 2304 (1997).
- [9] Z. Neufeld, *Phys. Rev. Lett.* **87**, 108301 (2001); Z. Neufeld, C. López, E. Hernández-García, and O. Piro, *Phys. Rev. E* **66**, 066208 (2002).
- [10] G. Karolyi, I. Scheuring, and T. Czaran, *Chaos* **12**, 460 (2002); E. Hernandez-Garcia et al., to appear in the Proceedings of the 2001 ISSAOS School on Chaos in Geophysical Flows.
- [11] P. H. Haynes, in *Proceedings of the NATO Advanced Study Institute on Mixing: Chaos and Turbulence*, edited by H. Chat'e and E. Villermaux (Kluwer Academic, Dordrecht, 1996), pp. 229–272.
- [12] D. G. H. Tan, P. H. Haynes, A. R. MacKenzie, and J. A. Pyle, *J. Geophys. Res. [Atmos.]* **103**, 1585 (1998).
- [13] E. R. Abraham and M. M. Bowen, *Chaos* **12**, 373 (2002).
- [14] I. Z. Kiss et al., *Physica D* **176**, 67 (2003); **183**, 175 (2003).
- [15] H. Aref, *J. Fluid Mech.* **143**, 1 (1984).
- [16] J. M. Ottino, *The Kinematics of Mixing: Stretching, Chaos and Transport* (Cambridge University Press, Cambridge, 1989).
- [17] S. Wiggins, *Chaotic Transport in Dynamical Systems* (Springer, New York, 1992).
- [18] Z. Neufeld, C. López, and P. Haynes, *Phys. Rev. Lett.* **82**, 2606 (1999).
- [19] Z. Neufeld, C. López, E. Hernandez-Garcia, and T. Tél, *Phys. Rev. E* **61**, 3857 (2000).
- [20] Z. Neufeld, *Phys. Rev. Lett.* **87**, 108301 (2001).
- [21] Z. Neufeld, P. H. Haynes, V. Garcon, and J. Sudre, *Geophys. Res. Lett.* **29**, 1534 (2002).
- [22] W. R. Young, A. J. Roberts, and G. Stuhne, *Nature (London)* **412**, 328 (2001).
- [23] N. M. Schnerb, Y. Louzoun, E. Bettelheim, and S. Solomon, *Proc. Natl. Acad. Sci. U.S.A.* **97**, 10322 (2000).
- [24] G. Falkovich, A. Fouxon, and M. G. Stepanov, *Nature (London)* **419**, 151 (2002).
- [25] M. R. Maxey and J. J. Riley, *Phys. Fluids* **26**, 883 (1983).
- [26] T. R. Auton, F. C. R. Hunt, and M. Prud'homme, *J. Fluid. Mech.* **197**, 241 (1988).
- [27] *Nonlinear Structure in Physical Systems* edited by L. Lam and H. C. Morris (Springer-Verlag, New York, 1990).
- [28] A. Crisanti, M. Falcioni, A. Provenzale, P. Tanga, and A. Vulpiani, *Phys. Fluids A* **4**, 1805 (1992).

- [29] P. Tanga and A. Provenzale, *Physica D* **76**, 202 (1994).
- [30] T. Elperin, N. Kleorin, and I. Rogachevskii, *Phys. Rev. Lett* **77**, 5373 (1996); T. Elperin et al, *Phys. Rev. E* **66**, 036302 (2002).
- [31] A. Bracco, P. H. Chavanis, A. Provenzale, and E. A. Spiegel, *Phys. Fluids* **11**, 2280 (1999).
- [32] A. Babiano, J. H. E. Cartwright, O. Piro, and A. Provenzale, *Phys. Rev. Lett.* **84**, 5764 (2000).
- [33] T. Shinbrot, M. M. Alvarez, J. M. Zalc, and F. J. Muzzio, *Phys. Rev. Lett.* **86**, 1207 (2001).
- [34] J. H. E. Cartwright, M. O. Magnasco, and O. Piro, *Chaos* **12**, 489 (2002).
- [35] I. J. Benczik, Z. Toroczkai, and T. Tél, *Phys. Rev. Lett.* **89**, 164501 (2002).
- [36] T. Nishikawa, Z. Toroczkai, and C. Grebogi, *Phys. Rev. Lett.* **87**, 038301 (2001).
- [37] T. Nishikawa, Z. Toroczkai, C. Grebogi, and T. Tél, *Phys. Rev. E* **65**, 026216 (2002).
- [38] Z. Liu, Y.-C. Lai, and J. M. Lopez, *Chaos* **12**, 417 (2002).
- [39] E. Balkovsky, G. Falkovich, and A. Fouxon, *Phys. Rev. Lett.* **86**, 2790 (2001).
- [40] C. Lopez, *Phys. Rev. E* **66**, 027202 (2002).
- [41] R. Reigada, F. Sagués, and J. M. Sancho, *Phys. Rev. E* **64**, 026307 (2001).
- [42] A. E. Motter and Y.-C. Lai, *Phys. Rev. E* **65**, 015205 (2002).
- [43] A. E. Motter, Y.-C. Lai, and C. Grebogi, *Phys. Rev. E* **68**, 056307 (2003).
- [44] Z. Toroczkai, G. Károlyi, A. Péntek, T. Tél, and C. Grebogi, *Phys. Rev. Lett.* **80**, 500 (1998).
- [45] G. Károlyi, A. Péntek, Z. Toroczkai, T. Tél, and C. Grebogi, *Phys. Rev. E* **59**, 5468 (1999).
- [46] Z. Neufeld, P. H. Haynes, and T. Tél, *Chaos* **12**, 426 (2002).
- [47] A. N. Zaikin and A. M. Zhabotinsky, *Nature (London)* **225**, 535 (1970).
- [48] F. A. Williams, *Combustion Theory: The Fundamental Theory of Chemically Reacting Flow Systems* (Benjamin-Cummings, Menlo Park, 1985).
- [49] B. B. Mandelbrot, *The Fractal Geometry of Nature* (W. H. Freeman, San Francisco, 1982).
- [50] K. Falconer, *Fractal Geometry: Mathematical Foundations and Applications* (Wiley, Chichester, 1990).
- [51] In systems with multifractality, we must replace D with the information dimension D_1 , because the advected particles only cover typical points of the fractal set.
- [52] A. N. Kolmogorov, I. G. Petrovski, and N. S. Piskunov, *Moscow Univ. Math. Bull.* **1**, 1 (1937), [English Translation appears in *Dynamics of curved Fronts*, Perspectives in Physics Series, edited by P. Pelce (Academic, New York, 1998)].
- [53] R. A. Fischer, *Proc. Annu. Symp. Eugen. Soc.* **7**, 355 (1937).
- [54] A. Mahadevan and D. Archer, *J. Geophys. Res., [Atmos.]* **105**, 1209 (2000).
- [55] After normalizing by the time scale of the flow, there are four relevant dimensionless parameters that are independent in the problem: the Stokes time (St), the Lagrangian time scale ($\sim 1/\lambda$), the diffusion time scale ($\sim 1/\kappa$), and the reaction time scale ($\sim 1/v_r$). The diffusion time scale is much longer than the others, but it does not appear explicitly in our approach (only via v_r). In terms of the other time scales, the condition for strong enhancement is the slow front propagation on the Lagrangian time scale.
- [56] R. Reif, *Statistical Physics* (McGraw-Hill, New York, 1967).
- [57] The Basset history term is neglected here since it is expected to be important only if the particle returns to previously visited sites, which is not the case for rising or descending particles under gravitational force ($-\mathbf{w}\mathbf{n}$) [see E. E. Michaelides, *J. Fluids Eng.* **119**, 233 (1997)].
- [58] Y.-T. Lau, J. M. Finn, and E. Ott, *Phys. Rev. Lett.* **66**, 978 (1991).

This figure "figure1.jpg" is available in "jpg" format from:

<http://arxiv.org/ps/nlin/0406011v1>

This figure "figure3.png" is available in "png" format from:

<http://arxiv.org/ps/nlin/0406011v1>